cmgh
CELLULAR AND MOLECULAR GASTROENTEROLOGY AND HEPATOLOGY

ORIGINAL RESEARCH

Intestinal Dysbiosis Contributes to the Delayed Gastrointestinal Transit in High-Fat Diet Fed Mice

Mallappa Anitha,[1,*] François Reichardt,[2,3] Sahar Tabatabavakili,[2,3] Behtash Ghazi Nezami,[2,3] Benoit Chassaing,[4] Simon Mwangi,[2,3] Matam Vijay-Kumar,[5,‡] Andrew Gewirtz,[4] and Shanthi Srinivasan[2,3]

[1] Department of Veterinary and Biomedical Sciences, The Pennsylvania State University, University Park, Pennsylvania; [2]Department of Digestive Diseases, Emory University School of Medicine, Atlanta, Georgia; [3]Atlanta VA Medical Center, Decatur, Georgia; [4]Center for Inflammation, Immunity and Infection, Institute for Biomedical Sciences, Georgia State University, Atlanta, Georgia; [5] Department of Nutritional Sciences & Medicine, The Pennsylvania State University, University Park, Pennsylvania

SUMMARY

High-fat diet feeding leads to intestinal dysbiosis and delayed colonic motility. Circulating lipopolysaccharide and palmitate act together to activate Toll-like receptor 4, leading to enteric neuronal apoptosis. Prebiotic supplementation reduces serum lipopolysaccharide and improves high-fat diet–induced nitrergic myenteric neuron degeneration and colonic transit delay.

BACKGROUND & AIMS: High-fat diet (HFD) feeding is associated with gastrointestinal motility disorders. We recently reported delayed colonic motility in mice fed a HFD for 11 weeks. In this study, we investigated the contributing role of gut microbiota in HFD-induced gut dysmotility.

METHODS: Male C57BL/6 mice were fed a HFD (60% kcal fat) or a regular/control diet (RD) (18% kcal fat) for 13 weeks. Serum and fecal endotoxin levels were measured, and relative amounts of specific gut bacteria in the feces were assessed by real-time polymerase chain reaction. Intestinal transit was measured by fluorescent-labeled marker and a bead expulsion test. Enteric neurons were assessed by immunostaining. Oligofructose (OFS) supplementation with RD or HFD for 5 weeks also was studied. In vitro studies were performed using primary enteric neurons and an enteric neuronal cell line.

RESULTS: HFD-fed mice had reduced numbers of enteric nitrergic neurons and showed delayed gastrointestinal transit compared with RD-fed mice. HFD-fed mice had higher fecal Firmicutes and *Escherichia coli* and lower Bacteroidetes compared with RD-fed mice. OFS supplementation protected against enteric nitrergic neuron loss in HFD-fed mice, and improved intestinal transit time. OFS supplementation resulted in a reduction in fecal Firmicutes and *Escherichia coli* and serum endotoxin levels. In vitro, palmitate activation of TLR4 induced enteric neuronal apoptosis in a Phospho–c-Jun N-terminal kinase–dependent pathway. This apoptosis was prevented by a c-Jun N-terminal kinase inhibitor and in neurons from *TLR4*$^{-/-}$ mice.

CONCLUSIONS: Together our data suggest that intestinal dysbiosis in HFD-fed mice contribute to the delayed intestinal motility by inducing a TLR4-dependent neuronal loss. Manipulation of gut microbiota with OFS improved intestinal motility in HFD mice. *(Cell Mol Gastroenterol Hepatol 2016;2:328–339; http://dx.doi.org/10.1016/j.jcmgh.2015.12.008)*

Keywords: Myenteric Neurons; Palmitate; Gut Microbiota; LPS; TLR4; Colon Transit.

Previous research has shown that high-fat diet (HFD) intake can lead to gastrointestinal complications such as constipation. Constipation can contribute significantly to the US health care expenditure, with approximately 5.8 million ambulatory patient visits and a $235 million annual expenditure.[1] Symptoms of constipation may be secondary to disease of the colon (stricture, cancer, anal fissure, proctitis), neurologic disorders (Parkinson's, spinal cord lesions), metabolic disturbances (diabetes mellitus, hypothyroidism, hypercalcemia), or caused by disordered colonic/pelvic floor function.[2] Risk factors for constipation include lower socioeconomic status, less physical activity, medication, depression, and stressful life events.[3] Excessive dietary fat intake correlates with constipation and prolonged colonic transit times.[4,5] Normal intestinal motility involves coordinated functioning of the extrinsic innervation of the intestine, the enteric nervous system, the longitudinal and circular muscles, as well as the interstitial cells of Cajal.[6] Diets rich in fat are associated with gastrointestinal motility disorders.[7,8] Rats fed a cafeteria diet rich in fat have been

*Current address of M.A.: Department of Veterinary and Biomedical Sciences, The Pennsylvania State University, University Park, Pennsylvania; ‡Current address of M.V.-K.: Department of Nutritional Sciences and Medicine, The Pennsylvania State University, University Park, Pennsylvania.

Abbreviations used in this paper: FITC, fluorescein isothiocyanate; HEK, human embryonic kidney; HFD, high-fat diet; IM-PEN, immortal postnatal enteric neuronal; JNK, c-Jun N-terminal kinase; LCM, laser capture microdissection; LPS, lipopolysaccharide; nNOS, neuronal nitric oxide synthase; OFS, oligofructose; PBS, phosphate-buffered saline; PCR, polymerase chain reaction; RD, regular/control diet; SAPK, stress-activated protein kinase; TLR, Toll-like receptor; WT, wild-type.

Most current article

2352-345X
http://dx.doi.org/10.1016/j.jcmgh.2015.12.008

shown to have longer overall gastrointestinal transit time.[9] We recently showed that mice fed a HFD have delayed intestinal motility associated with apoptosis of colonic enteric neurons and mitochondrial damage.[10]

In addition, HFD also alters the gut microbiota,[11] leading to an increase in the *Firmicutes* to *Bacteroidetes* ratio, which is associated with chronic metabolic endotoxemia.[12] Altering microbiota can lead to increased intestinal transit and electrogenic activity in neurons.[13] In a study involving women in whom a prebiotic dairy product was administered, there was reduced orocecal transit time owing to an increase in gut *Bifidobacterium*[14] and administration of *Bifidobacterium* improved defecation frequency in human beings.[15] *Bifidobacterium* can be increased in the gut by feeding dietary oligofructose (OFS) in mice.[16] In a study comparing patients with irritable bowel syndrome with healthy controls, an increase in the *Firmicutes* to *Bacteroidetes* ratio was observed,[17,18] potentially contributing to symptoms such as constipation in irritable bowel syndrome patients.[19,20]

Gut microbial products signal through the pathogen recognition Toll-like receptor (TLR) family. In the murine enteric nervous system, TLR4 expression is maximal in the distal colon[21] and TLR3, 4, and 7 have been shown to be expressed in myenteric neurons and glia cells.[22] TLRs have been implicated in neuronal apoptosis,[23] and excess TLR4 activation by lipopolysaccharide (LPS) activates proinflammatory pathways and cytokine release within enteric neurons.[24,25] A HFD can lead to increased TLR4 expression and signaling.[26] Moreover, saturated fatty acids such as palmitate, a major fatty acid in HFD, can activate TLR4 signaling,[27,28] and hyperlipidemia leads to TLR4-dependent renal damages.[29]

The effects of HFD and LPS together on the enteric nervous system is not known. Because a HFD increases circulating LPS and can impact TLR4 signaling in the gut we hypothesized that the enteric neuronal alteration induced by the HFD feeding is dependent on TLR4 activation. Thus, we examined the changes in gut microbiota in HFD-fed mice and the effects of OFS supplementation on myenteric neurons and gastrointestinal motility. In addition, we examined in vitro the effect of excess saturated fatty acids on TLR4 expression in enteric neurons and investigated the subsequent enteric neuronal damage.

Materials and Methods

Animals

Eight-week-old male C57BL/6J mice obtained from Jackson Laboratories (Bar Harbor, ME) were fed a HFD (60% calories from fat, Teklad Diet 06414) or regular/control diet [RD] (18% calories from fat) for 13 weeks. The HFD was purchased from Harlan Laboratories, Inc (Madison, WI). Mice were divided into 4 groups and fed for another 5 weeks with or without OFS supplementation in the drinking water (0.125 g/mL).[30] OFS (Orafti P95) was purchased from Beneo (Mannheim, Germany). Throughout the experiment, mice were monitored for body weight and stool indices. All animal studies were approved by the Institutional Animal Care and Use Committee at Emory University.

Reagents

The following reagents were obtained: human embryonic kidney (HEK)-Blue-mTLR4 cells (Invivogen, San Diego, CA), Quanti-Blue medium (Invivogen), *Escherichia coli* LPS (Sigma, St. Louis, MO), Histogene laser capture microdissection (LCM) staining kit and Picopure RNA isolation kit (Arcturus; Life Technologies Corporation, Carlsbad, CA), Sensiscript RT kit, QIAamp DNA Stool Mini Kit, and QuantiFast SYBR Green Polymerase Chain Reaction (PCR) Kit (Qiagen, Valencia, CA), and stress-activated protein kinase/c-Jun N-terminal kinase (JNK) inhibitor (SP600125; Sigma Aldrich, St. Louis, MO). All other reagents were obtained from Sigma.

Antibodies and Primers

The following antibodies were obtained: neuronal nitric oxide synthase (nNOS) and peripherin (Millipore, Billerica, MA), Phospho-c-Jun N-terminal kinase, and cleaved caspase-3 (Cell Signaling Technology, Danvers, MA), β-actin (Sigma), and Alexa Fluor secondary antibodies (Life Technologies Corp, Waltham, MA). All oligonucleotide primers were purchased from Integrated DNA Technologies (IDT, Coralville, IA).

Measurement of LPS in Serum

The concentration of LPS in mouse serum was detected by using the Limulus Ameobocyte Lysate assay according to the instructions provided by the manufacturer (Lonza, Walkersville, MD). The endotoxin concentration of the serum samples was measured by plotting endotoxin standard graph (0.1–1.0 EU/mL), using standards provided in the kit.

Fecal LPS Load Quantification

Fecal LPS was quantified using HEK-Blue-mTLR4 cells. Feces suspension was prepared in phosphate-buffered saline (PBS) to a final concentration of 100 mg/mL and homogenized for 10 seconds using a Mini-Beadbeater-24 (without beads to avoid bacteria lysis). Samples then were centrifuged for 2 minutes at 8000 *g*. The supernatant was serially diluted, and applied to HEK-mTLR4 mammalian cells. Purified *E coli* LPS was used as a positive control and for preparation of the standard curve. After a 24-hour stimulation, cell culture supernatant was applied to Quanti-Blue medium, and alkaline phosphatase activity was measured at 620 nm after 30 minutes as previously described.[31]

PCR Microarray

PCR arrays were performed using the PAMM-018ZA mouse TLR Signaling Pathway RT[2] Profiler PCR Array (Qiagen). This array profiles the expression of 84 genes coding for members of the TLR signaling family (Tlr1–9); TLR adaptor and effector proteins; signaling pathways downstream of TLR activation (nuclear factor-κB, JNK/p38, interferon regulatory factor, and Janus kinase/signal transducers and activators of transcription signaling pathways); molecules associated with bacterial, viral, fungal, and parasitic-specific responses; and those associated with the regulation of adaptive immunity. Briefly, colonic myenteric ganglia from 3 control mice and 3 HFD-fed mice were

captured by laser capture microdissection as previously described.[32] PCR arrays were performed according to the recommended procedure using complementary DNA prepared as previously described[32] from total RNA isolated from the captured myenteric ganglia using the Picopure RNA isolation kit and pooled by treatment group.

Quantitative PCR

Bacterial total DNA (genomic DNA) was isolated from RD and HFD mice stool using the QIAamp DNA Stool Mini Kit. Quantitative PCR was performed using the following oligonucleotide primers: Bacteroidetes (forward) 5'-GAAG GTCCCCCACATTG-3' and Bacteroidetes (reverse) 5'-CGCKA CTTGGCTGGTTCAG-3'; *E coli* (forward) 5'-CATGCCGCGTG TATGAAGAA-3' and *E coli* (reverse) 5'-CGGGTAACGTCAAT GAGCAAA-3'; Bifidobacteria (forward) 5'-CGGGTGAGTAAT GCGTGACC-3' and Bifidobacteria (reverse) 5'-TGATAGGAC GCGACCCCA-3'; Firmicutes (forward) 5'-GGAGYATGTGGTTT AATTCGAAGCA-3' and Firmicutes (reverse) 5'-AGCTGACG ACAACCATGCAC-3'; total bacteria (forward) 5'-ACTCCTACG GGAGGCAG-3' and total bacteria (reverse) 5'-GTATTACCG CGGCTGCTG-3'.

Two thirds of each reaction was analyzed on a 1.5% agarose gel stained with ethidium bromide, and the amplified products were visualized by ultraviolet trans-illumination.

Quantification of Bacterial Load in Stool by Quantitative Real-Time PCR

Bacterial total DNA (genomic DNA) was isolated from RD and HFD mice stool, treated with or without OFS, using the QIAamp DNA Stool Mini Kit. For real-time PCR, amplifications were detected using the QuantiFast SYBR Green PCR Kit in reactions performed as previously described.[33] Total bacteria was used as an endogenous control to normalize the target gene expression.

Whole-Mount Tissue Staining

Longitudinal muscle strips with intact myenteric ganglia, from the proximal colon of RD and HFD mice treated with or without OFS, were dissected carefully from the remaining colonic tissue and fixed in 4% paraformaldehyde as previously published[10,32]; blocked for 1 hour in PBS containing 0.3% Triton X-100 (BioRad, Hercules, CA) and 5% normal donkey serum; and incubated with rabbit peripherin (1:500), or rabbit nNOS (1:200) antibodies in PBS containing 1.5% normal donkey serum, 0.3% Triton X-100, and 0.01% sodium azide, for 72 hours at room temperature. Secondary detection was performed by incubation with anti-rabbit IgG (1:200) conjugated to Alexa Fluor 594 antibody. Five fields per mouse colon were evaluated randomly for statistics.

Total Gastrointestinal Transit Time

Mice were gavaged with 0.1 mL of a semiliquid solution containing 5% Evans blue in 0.9% NaCl with 0.5% methyl cellulose, and the time for expulsion of the first blue pellet was determined. This test was performed in the last week of the experiment.

Small Intestinal Transit Time

Small intestinal transit was determined by assessing the distribution of 70-kilodalton fluorescein isothiocyanate (FITC)-conjugated dextran in the intestines of mice as described previously.[34] Transit was analyzed using the intestinal geometric center of the distribution of FITC-conjugated dextran throughout the intestine, and was calculated as previously described.[35]

Colonic Transit Time

A 3-mm glass bead was placed 2 cm proximal to the anal opening using a plastic Pasteur pipette lightly lubricated with lubricating jelly. Distal colonic transit time was assessed by measuring the amount of time between bead placement and expulsion of the bead. The test was performed in the last week of the diet.

Neuronal Cell Preparation

The intestines of embryos from embryonic day 13.5 pregnant wild-type (WT) and *TLR4*$^{-/-}$ mice were used for the enteric neuronal preparation as described previously, with slight modification of the protocol as mentioned.[36]

Immortal Postnatal Enteric Neuronal Cell Line Culture

The immortal postnatal enteric neuronal (IM-PEN) cell line[37] was seeded onto 6-well plates with modified N2 medium containing glial cell line-derived neurotrophic factor (100 ng/mL), 10% fetal bovine serum, and 20 U/mL of recombinant mouse interferon-γ, and were cultured in a humidified tissue culture incubator containing 10% CO_2 at permissive temperature, 33°C. After 48 hours the medium was changed to Neurobasal-A medium containing B-27 serum-free supplement, 1 mmol/L glutamine, 1% fetal bovine serum, GDNF (100 ng/mL), and the plates were transferred to an atmosphere of 5% CO_2 at 39°C. Palmitate was used in 0.5–1 mmol/L concentrations, which is within the physiologically increased limits observed in human beings and animals, and can induce insulin resistance and hyperlipidemia-associated complications.[38] Palmitate was dissolved in isopropanol to obtain a stock concentration of 100 mmol/L. The required volume of the stock was added to the medium for 24-hour incubations. For SAPK/JNK inhibitor experiments cells were preincubated with 20 mmol/L SP600125 for 2 hours before addition of palmitate.

Quantitative Reverse-Transcription PCR

IM-PEN cells were cultured for 24 hours in Neurobasal-A medium in the presence or absence of palmitic acid (0.5 and 1 mmol/L) in 6-well plates. Total RNA was isolated using the RNeasy Mini Kit (Qiagen) and was used to synthesize first-strand complementary DNA using the Sensiscript RT Kit and RT^2 SYBR Green ROX qPCR Mastermix (Qiagen) according to the recommended procedure; reverse-transcription PCR was performed using the following oligonucleotide primers: peripherin (forward) 5'-ACAACCTG GTGCTCTTCCGTA-3' and peripherin (reverse) 5'-TCTGGC

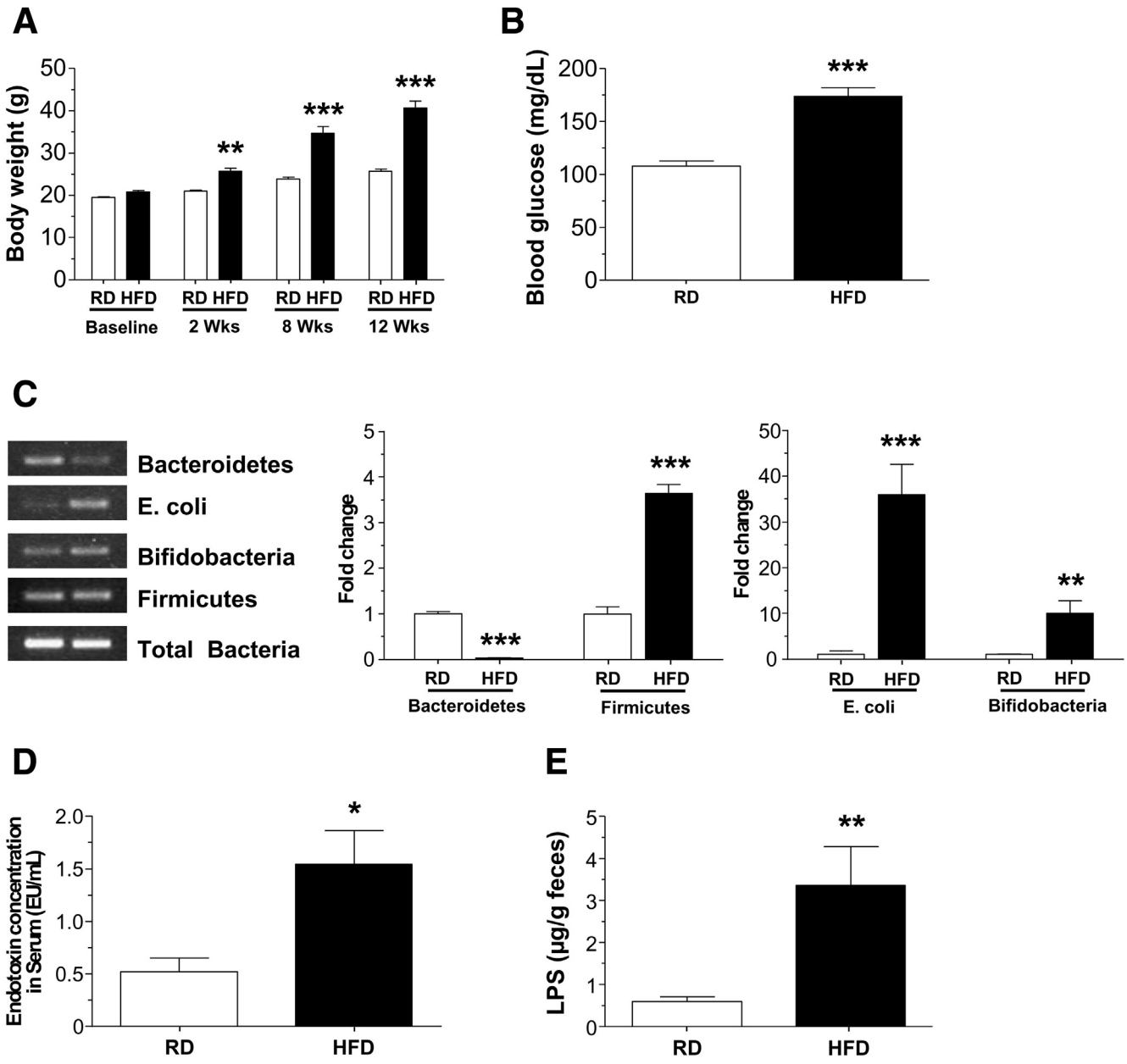

Figure 1. High-fat diet feeding alters gut microbiota and results in endotoxemia in mice. (*A*) Body weights of mice fed a HFD or RD for up to 12 weeks and (*B*) fasting blood glucose level after 12 weeks. (*C*) PCR analyses of gut microbiota in stool from HFD- and RD-fed mice stool showing the relative amount of Bacteroidetes, Firmicutes, *E coli*, and Bifidobacteria. (*D*) Serum endotoxin levels and (*E*) stool LPS levels in RD- and HFD-fed mice. Results are means ± SEM; n = 12 per group. $^{*}P < .05$, $^{**}P < .01$, and $^{***}P < .001$.

TTCACTGTTGCCTCT-3'; TLR4 (forward) 5'-TCAGCTTTGGT CAGTTGGCTCT-3' and TLR4 (reverse) 5'-AGACCCATGAAG TTGGCACTCA-3'; glyceraldehyde-3-phosphate dehydrogenase (forward) 5'-CCAGTATGATTCTACCCACGGCAA-3' and glyceraldehyde-3-phosphate dehydrogenase (reverse) 5'-ACAGTCTTCTGAGTGGCAGTGATG-3'.

LCM

Myenteric ganglia were dissected by LCM, as previously described,[34] and RNA were isolated from the ganglia using standard isolation techniques as previously described.[10]

Western Blot

Western blot analysis was performed according to standard methods as previously described.[39] Cell lysates obtained from IM-PEN cells treated with or without palmitate (0.5–1 mmol/L) for 24 hours were used to probe for P-JNK, and cleaved caspase-3 with respective specific antibodies by Western blot analysis. β-actin was used as a loading control. A semiquantitative measurement of the band intensity was performed using the Scion Image computer software program (Bethesda, MD) and expressed as a ratio of band intensity with respect to the loading control.

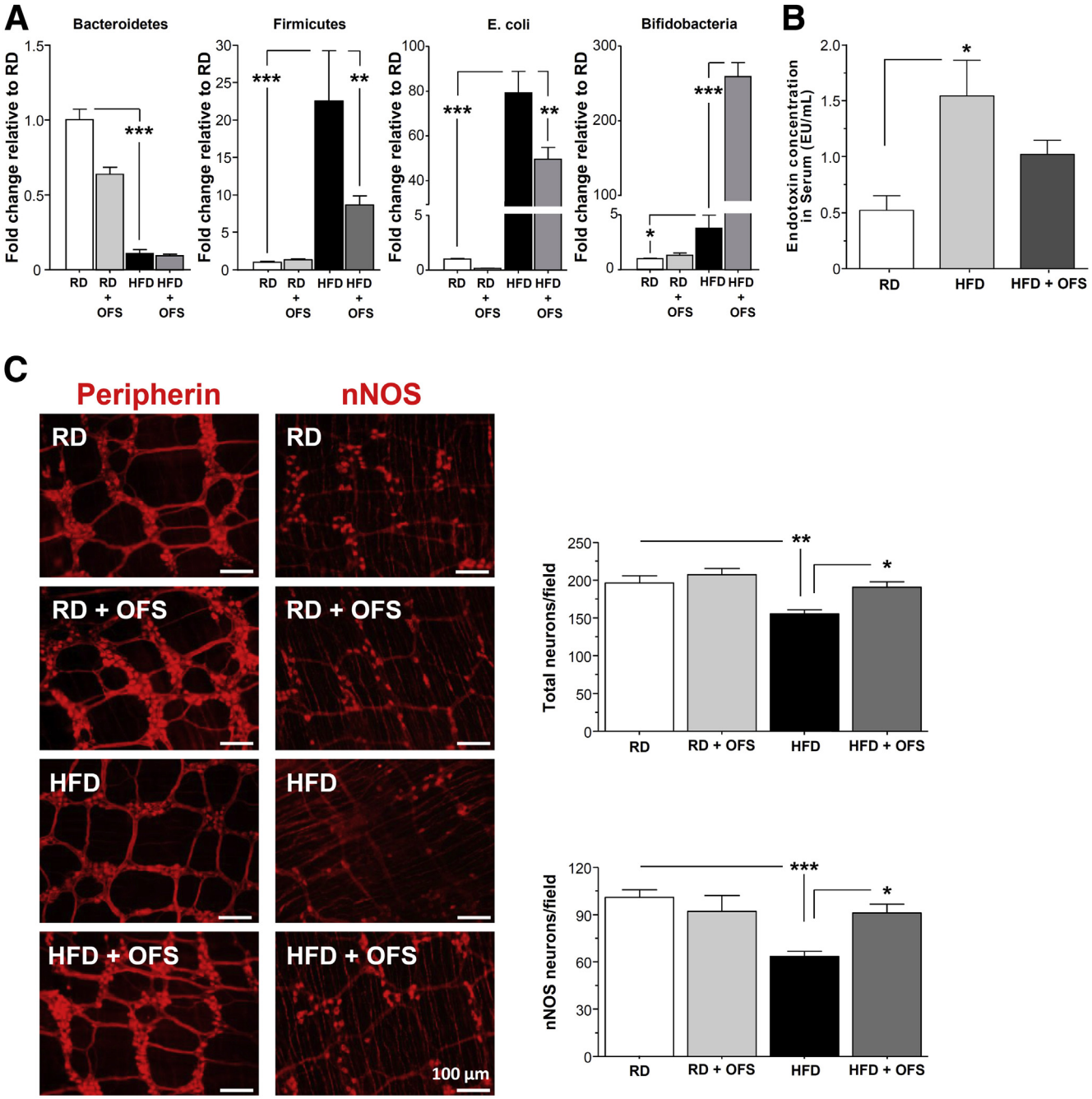

Figure 2. OFS-induced changes in gut microbiota leads to reversal of HF-diet induced enteric neuronal loss. (*A*) Gut microbiota in stool from mice fed HFD or RD supplemented with or without OFS. (*B*) Endotoxin levels in serum from mice fed HFD or RD supplemented with or without OFS. (*C*) Representative photographs of proximal colon whole mount stained for peripherin and *nNOS* and histograms of neuronal counts. The number of stained neurons was determined per unit area. *Scale bars*: 50 μm. Results are means ± SEM; n = 6. *$P < .05$, **$P < .01$, and ***$P < .001$.

In Vitro Neuronal Apoptosis

Apoptosis was measured in cultured primary enteric neurons after 24 hours of incubation with palmitate (0.5 mmol/L) and/or LPS (1 μg/mL) by quantifying cleaved caspase-3–positive primary neurons from WT and *TLR4*$^{-/-}$ mice (2-day-old pups). Approximately 100 neurons were scored for each condition.

Statistical Analysis

Statistics were performed with the Student *t* test or with 1-way analysis of variance (GraphPad software; GraphPad, Inc, La Jolla, CA). A *P* value of .05 or less was considered statistically significant.

All authors had access to the study data and reviewed and approved the final manuscript.

Results

High-Fat Diet Alters Gut Microbiota and Results in Endotoxemia

HFD-fed mice gained significantly more weight compared with the RD group ($P < .001$) (Figure 1*A*), and had higher fasting blood glucose levels ($P < .001$) (Figure 1*B*). A HFD has been reported to alter microbiota composition, specifically reducing the proportion of Bacteroidetes and increasing the proportion of Firmicutes. To investigate if this held true in our colony of mice, we measured the relative amounts of these phyla by real-time polymerase chain reaction (qPCR). We observed that the HFD mice had a statistically significant reduction in Bacteroidetes ($P < .001$) and a significant increase in Firmicutes, Bifidobacteria, and *E coli* ($P < .001$) relative to mice fed a RD (Figure 1*C*), indicating the diet altered the microbiota as expected. As reported in Figure 1*D*, the endotoxin level in serum was higher in HFD-fed mice ($P < .05$), which correlated with increased stool endotoxin level ($P < .01$) (Figure 1*E*) compared with RD-fed mice.

OFS Supplementation Leads to Changes in Gut Microbiota and Ameliorates HFD-Induced Enteric Neuronal Changes

Because HFD was associated with altered gut microbiota including increased gram-negative bacteria *E coli* and increased endotoxemia, we investigated the role of prebiotics on gut microbiota composition, endotoxemia, gastrointestinal motility, and enteric neurons. Mice fed a RD or HFD were supplemented with or without OFS for 5 weeks. OFS supplementation caused a robust increase in Bifidobacteria ($P < .001$), with a significant decrease in Firmicutes and *E coli* level ($P < .01$) in HFD-fed mice (Figure 2*A*). As seen in Figure 2*B*, OFS decreased the level of endotoxemia in HFD-fed mice. We next investigated the impact of HFD and OFS supplementation on myenteric neurons. HFD mice showed a reduced number of enteric neurons after 18 weeks of feeding that was associated with a loss of nitrergic neurons. As seen in Figure 2*C*, supplementation with OFS for 5 weeks was sufficient to restore the HFD-induced neuronal loss ($P < .05$).

OFS Supplementation Leads to Reversal of HFD-Induced Intestinal Dysmotility

Based on our observation that OFS supplementation reversed the effects of HFD feeding on enteric neuronal damage, we next examined the effect of OFS on HFD-induced delayed intestinal motility. HFD resulted in a longer total intestinal transit time measured by Evans blue gavage compared with RD ($P < .001$) (Figure 3*A*). Distal colonic motility as measured by the bead expulsion time was longer in the HFD group, indicating slower colonic propulsion compared with RD ($P < .01$) (Figure 3*B*). OFS supplementation improved the intestinal motility as assessed by Evans blue gavage and the bead expulsion time ($P < .01$). Relative distribution of FITC-conjugated dextran fluorescence to examine small intestinal transit also was found to be delayed in HFD mice, as noted by a significantly lower intestinal geometric center ($P < .05$) (Figure 3*C*), and supplementation with OFS was sufficient to restore normal small-intestine transit ($P < .05$).

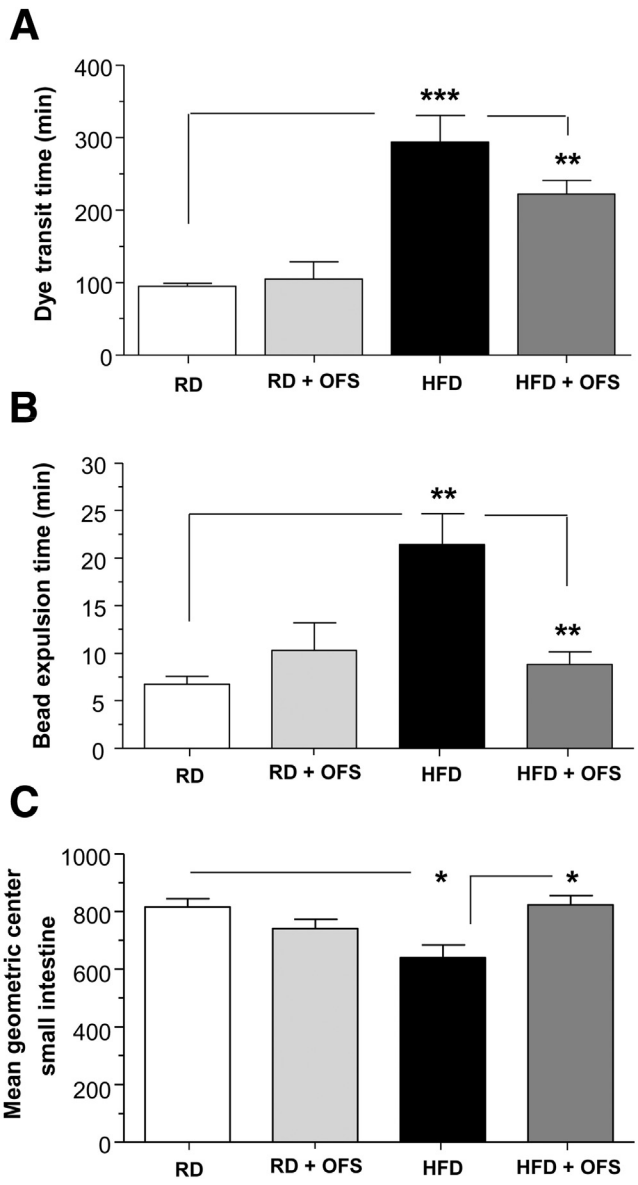

Figure 3. OFS supplementation leads to reversal of HFD-induced intestinal dysmotility. Assessment of gastrointestinal motility in mice fed a RD or HFD for 13 weeks and an additional 5 weeks with the diet supplemented with or without OFS. (*A*) Dye transit time after oral gavage with Evans blue dye/methyl cellulose solution, (*B*) bead expulsion time, and (*C*) mean geometric center of small intestine in mice fed a RD or HFD for 13 weeks and an additional 5 weeks with the diet supplemented with or without OFS. Results are means ± SEM; n = 6. *$P < .05$, **$P < .01$, and ***$P < .001$.

HFD Induced Increased Expression of TLR4 and its Downstream Targets in Enteric Ganglia

We next determined if a diet high in fat could cause an alteration in TLR4 expression. Expression of TLR4 and its

A

Gene Symbol	HFD-induced fold upregulation
Cd80	12.996
Cd86	7.1107
Cebpb	45.8866
Eif2ak2	20.2521
Hspa1a	6.4531
Il6ra	6.8211
Irak1	4.1125
Ly86	9.1261
Map3k7	13.1775
Mapk8	112.986
Mapk8ip3	7.2602
Peli1	89.8845
Tlr2	5.579
Tlr4	18.6357
Tlr5	6.9163
Tollip	5.7757
Ube2n	22.6274

B

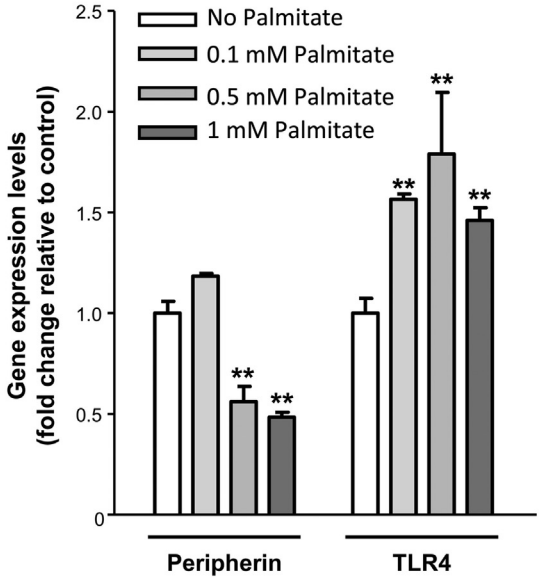

Figure 4. HFD feeding increases the expression of TLR4 and its downstream target genes in myenteric ganglia. (*A*) List of highly up-regulated genes in myenteric ganglia isolated by laser capture microdissection from the proximal colon of mice fed RD or HFD for 13 weeks (n = 3). (*B*) Effect of palmitate on peripherin, and TLR4 gene expression in the IM-PEN cell line as assessed by real-time PCR. Results are means ± SEM; n = 3. $^{**}P < .01$.

A

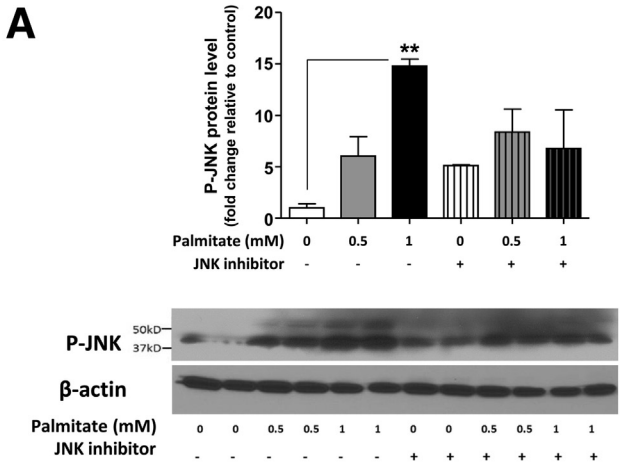

B

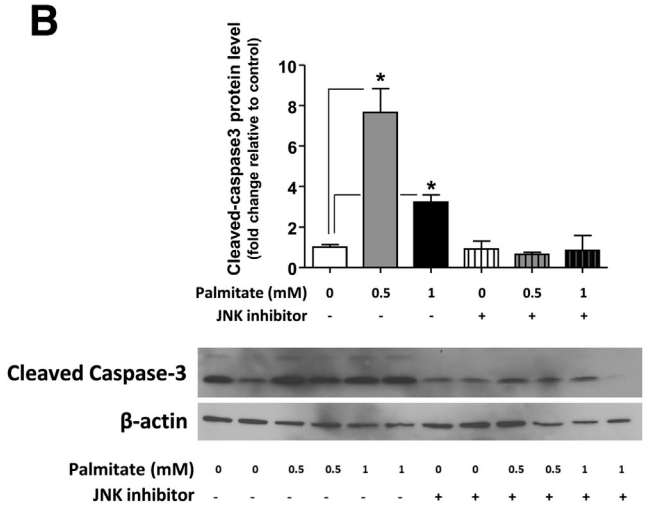

Figure 5. Palmitate induces the phosphorylation of JNK and cleavage of caspase-3 in enteric neurons in vitro. Western blot analysis of (*A*) JNK phosphorylation and (*B*) caspase-3 cleavage in IM-PEN neuronal cells cultured in medium supplemented with various concentrations of palmitate in the absence or presence of the JNK inhibitor SP600125. Plotted are means ± SEM; n = 3. $^{*}P < .05$, $^{**}P < .01$.

downstream targets was determined in LCM-isolated RNA from myenteric ganglia in conjunction with a PCR microarray analysis focusing on TLR4 and its target genes. As seen in Figure 4*A*, there was an increase in the expression of TLR4 and genes involved in the TLR4 signaling (mitogen-activated protein kinase, Peli1) in myenteric ganglia of HFD-fed mice compared with RD-fed mice. Because HFD are rich in saturated fats, we next examined the contribution of palmitate on this alteration of TLR4 signaling. We observed in vitro that 24-hour incubation with increasing concentration of palmitate enhanced the TLR4 expression in the IM-PEN cell line concurrently with a decrease of peripherin expression, suggesting enteric neuronal cell loss (Figure 4*B*).

Role of the TLR4 and SAPK/JNK Signaling Pathway in Palmitate-Induced Neuronal Apoptosis

To understand the mechanism of palmitate-induced enteric neuronal apoptosis, we evaluated the role of the JNK signaling pathway using Western blot analysis. We examined the activation of JNK in the IM-PEN cell line cultured in the presence and absence of palmitate and a specific inhibitor of the SAPK/JNK signaling pathway, namely SP600125, which blocks the activity of JNK1, JNK2,

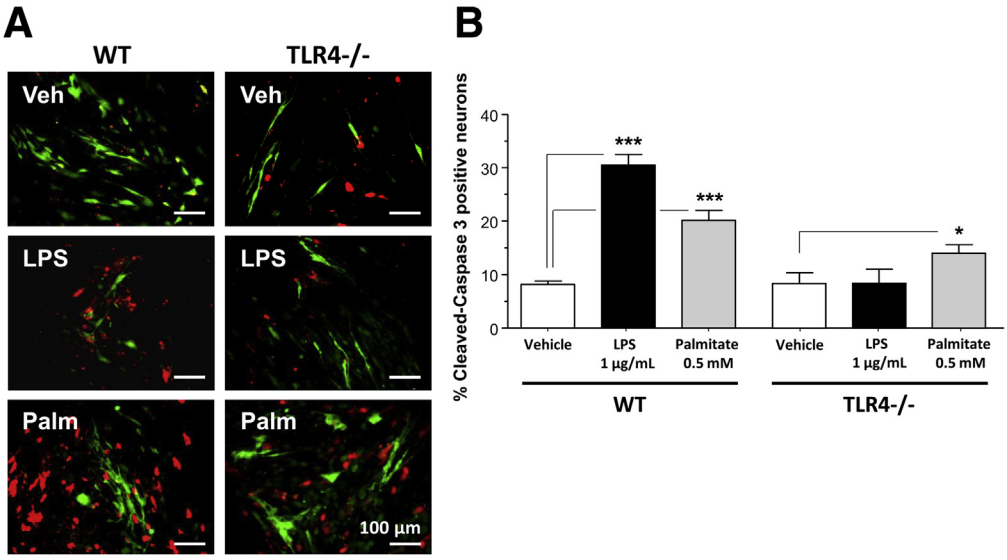

Figure 6. Effect of palmitate on the survival of primary enteric neuronal cells from WT and TLR4$^{-/-}$ mice. (*A*) Representative photographs of WT or *TLR4*$^{-/-}$ primary enteric neuronal cells cultured in the presence of vehicle, LPS (1 μg/mL), or palmitate (0.5 mmol/L), and stained for PGP9.5 (green) and cleaved-caspase-3 (red). (*B*) Plot of cleaved caspase-3–positive neuronal cell counts. Plotted are means ± SEM; n = 6–8. **P* < .05, ****P* < .001. Palm, palmitate; Veh, vehicle.

and JNK3. Western blot analysis showed that palmitate incubation resulted in the activation of JNK as seen by a dose-dependent increase in phosphorylation of JNK (Figure 5*A*). In the presence of this inhibitor in the culture medium, palmitate-induced enteric neuronal JNK phosphorylation was prevented (Figure 5*A*). In these experiments, an increase of cleaved caspase-3 cleavage was observed with 0.5 and 1 mmol/L palmitate (Figure 5*B*), and this was prevented by the JNK inhibitor. To understand the role of palmitate in enteric neuronal loss, we evaluated apoptosis after 24-hour incubation with 0.5 mmol/L palmitate or 1 μg LPS in neurons from WT or *TLR4*$^{-/-}$ mice. In WT neurons, both LPS and palmitate significantly increased the proportion of neurons expressing cleaved caspase-3 (Figure 6*A* and *B*). Palmitate increased the cleaved caspase-3 expression in *TLR4*$^{-/-}$ neurons, but this increased expression was significantly less than that in WT neurons. Altogether, those data show that TLR4 activation in response to HFD feeding, both through endotoxemia and palmitate, leads to apoptosis in enteric neurons and subsequent delayed intestinal motility.

Discussion

Our results show that delayed intestinal motility in HFD-fed mice for 13 weeks is associated with an increased serum endotoxin level and a decreased proportion of myenteric nitrergic neurons in the proximal colon. Moreover, the restoration of the microbiota by OFS contributed to an improvement in gastrointestinal motility and enteric neuronal integrity. Finally, we showed that treatment with palmitate increased TLR4 expression and reduced neuronal survival in cell culture in a JNK-dependent pathway. Together our data suggest that HFD-induced intestinal dysbiosis contributes to the delayed intestinal motility by altering the colonic myenteric plexus.

High-fat feeding induces intestinal dysmotility in human beings and animal models,[40] in particular slow intestinal propulsive activity.[41] We reported recently that mice fed a HFD (60% calories from fat) for 12 weeks showed delayed gastrointestinal transit associated with a reduced number of nitrergic neurons in the proximal colon.[10] These results were confirmed in the present study in which mice fed a diet with the same fat content had a slower small intestinal transit, illustrated by a reduced mean geometric center, and also a reduced colonic transit associated with a smaller proportion of colonic nitrergic myenteric neurons. Deficits in myenteric NOS neurons may be associated with failure of colonic propulsion as seen in Hirschsprung's and Chagas' diseases,[42] but also in a Parkinson's disease model in which it was associated with a reduced fecal output.[43] Therefore, we hypothesize in this study that the loss of nitrergic myenteric neurons represents the major cause of the colonic motility leading to constipation in HFD-fed animals, although other neuronal alteration cannot be excluded and will be the topic of future studies. This loss of nitrergic myenteric neurons appears to be a common feature associated with long-term, high-fat feeding. Stenkamp-Strahm et al[44] described similar loss in the duodenum of mice presenting with symptoms of diabetes after the ingestion of a HFD (72% kcal fat) for 8 weeks, but it also was described in the colon of mice fed a moderately HFD (35% fat content) for 8 and 17 weeks.[45] Similar alterations were observed in the colon of mice fed with a low-fat diet (21% fat, 2% cholesterol) for 33 weeks, which showed hepatic steatosis but no signs of diabetes.[46] Several hypotheses have been proposed to explain the underlying factors for HFD leading to myenteric neurodegeneration including oxidative stress and changes in the microbiota.

It has been shown that a HFD markedly affects the composition of the intestinal microbiota.[47] This diet-induced dysbiosis leads to endotoxemia (ie, increased plasma LPS levels) and can contribute to diabetes development.[48] Therefore, we hypothesized that the alteration of the gut microbiota induced by chronic high-fat consumption may be

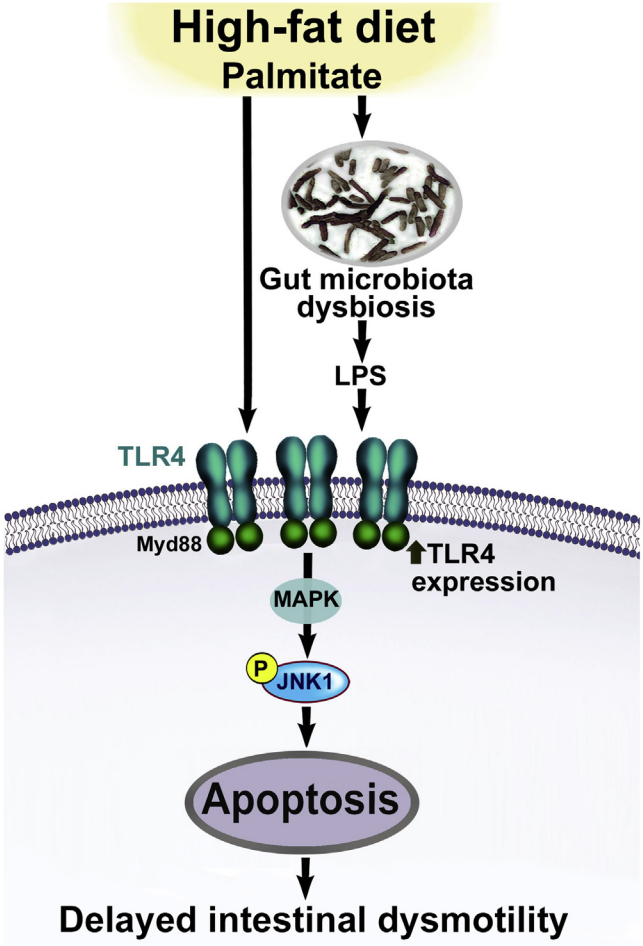

Figure 7. A proposed model by which enhanced TLR4 activation leads to myenteric neuronal apoptosis in HFD-fed mice. We propose that a HFD can lead to increased circulating LPS levels, resulting from gut microbiota dysbiosis and activation of TLR4 signaling. In addition, palmitate in HFD can lead to increased TLR4 expression. Together LPS and palmitate lead to enhanced TLR4 signaling, which in turn leads to enhanced mitogen-activated protein kinase (JNK1) signaling and apoptosis of myenteric neurons, and consequent delayed intestinal motility.

responsible for nitrergic myenteric neuropathy. We first characterized the fecal proportions of *Bacteroidetes* and *Firmicutes* that are known to be altered in obesity.[49] In our study, mice on a HFD for 13 weeks showed an increased *Firmicutes* to *Bacteriodetes* ratio, associated with an increased concentration of gram-negative bacteria (as *E coli*) in the stool. This intestinal dysbiosis led to increased fecal and also plasma LPS levels, which contributes to myenteric neuropathy as observed in cultured neurons.[50]

To understand the role of the gut microbiota in this alteration, HFD mice were supplemented with OFS for 5 weeks. Cani et al[16] showed that long-term OFS supplementation (10% of ingested food) increases the proportion of bifidobacteria and reduces endotoxemia. OFS supplementation in our study re-established the ratio of Firmicutes to Bacteroides and reduced plasma LPS after 5 weeks. Although the OFS supplementation in RD led to subtle changes in microbial composition, this was not associated with a significant change in neuronal numbers or intestinal motility. We found that the damaging effect of HFD on enteric neurons was reversed in the OFS-supplemented mice, raising the question of the origin of the new peripherin and nNOS-positive cells. Stem cells, glia, or existing neurons could be the source of these new cells and characterization of this myenteric neuronal renewal will be the topic of future studies in our laboratory.

To examine the mechanism of HFD-induced neuronal loss we focused on the role of saturated fatty acids such as palmitate, which can activate TLR4,[28] in conjunction with increased LPS. In vitro, both induce apoptosis in cultured myenteric neurons.[50,51] Moreover, palmitate increases TLR4 expression in pancreatic carcinoma cell lines.[52] The same study also observed a similar increase of TLR4 messenger RNA of pancreatic islets in mice fed for 24 weeks with a HFD (31.5% fat content). Therefore, we investigated in cultured enteric neurons the role of palmitate in the regulation of TLR4 expression. Our results showed that incubation with palmitate (in similar concentrations used by Voss et al[51]) reduces enteric neuronal survival as seen by reduced peripherin expression, and also increases TLR4 messenger RNA. Our study also confirmed that TLR4 activation, illustrated by the increase of JNK-1 phosphorylation (mitogen-activated protein kinase involved in the TLR4 pathway[53]), is required for apoptosis in enteric neurons incubated with palmitate because the specific deletion of this receptor ameliorated the increase of cleaved caspase-3 in the neurons. The activation of TLR4 downstream pathways appears to be critical in the palmitate-induced neuronal apoptosis because in vitro treatment with palmitate induced activation of JNK-1 by causing increased phosphorylation of JNK-1, which was associated with increased neuronal apoptosis. Addition of SP600125, which blocks the activity of JNK1, JNK2, and JNK3, helped to prevent palmitate-induced enteric neuronal apoptosis. It has been shown that TLR4 activation of JNK1/2 leads to neuronal death in primary cultures of rat cortical neurons.[54] Our data highlight a potential pivotal role for P-JNK in enteric neuronal apoptosis in response to TLR4 activation. Future studies will be required to define whether other alternative intracellular pathways can be involved in this neuronal cellular loss, such as the TLR4-phosphatidylinositol 3-kinase/protein kinase B (PKB) pathway that recently was described in hippocampal neuronal apoptosis.[55] In addition, our study has shown that the proinflammatory cytokine IL6 expression also was increased in myenteric ganglia from HFD mice, confirming the role of TLR4 in LPS-induced neuronal inflammation.[25]

We propose that the excess of HFD, containing palmitate, may chronically enhance the neuronal TLR4 signaling in the colonic myenteric plexus. Palmitate and LPS may act together on myenteric neurons, resulting in apoptosis that leads to motility disorders. We previously published that a lack of TLR4 expression leads to a reduction in nitrergic neurons.[32] In the present study we showed that excess TLR4 stimulation leads to neuronal apoptosis. It is already

known that optimal TLR4 signaling is essential for nitrergic neuronal development and survival in the enteric nervous system, in particular in the colon where its expression is enhanced.[21,22] The endotoxemia associated with a high-fat diet could initiate myenteric inducible NOS activation, known to increase in neurons after the systemic administration of LPS,[56] and can induce an overproduction of NO in nitrergic neurons, leading to oxidative stress and apoptosis.[42,57] This will be the focus of our future studies as we continue to understand the mechanisms of a HFD-induced nitrergic enteric neuronal degeneration and delayed colonic transit. One possibility is that the loss of nitrergic myenteric neurons leading to a reduction of the inhibitory tone can contribute to a hypercontractility, abnormal peristalsis, and subsequent constipation.

In conclusion, intestinal dysbiosis contributes to gastrointestinal motility disorders in HFD-fed mice through LPS-induced activation of TLR4 and JNK signaling pathways. Our findings suggest a novel mechanism of HFD and hyperlipidemia-induced enteric neuronal damage in a TLR4-dependent manner (Figure 7). This mechanism includes altered microbiota, increased endotoxemia, and subsequent enteric neuronal damage. This damage can be prevented by OFS and involves the TLR4 signaling pathways. This study can help identify novel targets for the treatment of gastrointestinal motility disorders.

References

1. Martin BC, Barghout V, Cerulli A. Direct medical costs of constipation in the United States. Manag Care Interface 2006;19:43–49.
2. Bharucha AE, Dorn SD, Lembo A, et al. American Gastroenterological Association medical position statement on constipation. Gastroenterology 2013; 144:211–217.
3. Bharucha AE, Pemberton JH, Locke GR 3rd. American Gastroenterological Association technical review on constipation. Gastroenterology 2013;144:218–238.
4. Taba Taba Vakili S, Nezami BG, Shetty A, et al. Association of high dietary saturated fat intake and uncontrolled diabetes with constipation: evidence from the National Health and Nutrition Examination Survey. Neurogastroenterol Motil 2015;27:1389–1397.
5. vd Baan-Slootweg OH, Liem O, Bekkali N, et al. Constipation and colonic transit times in children with morbid obesity. J Pediatr Gastroenterol Nutr 2011; 52:442–445.
6. Huizinga JD, Zarate N, Farrugia G. Physiology, injury, and recovery of interstitial cells of Cajal: basic and clinical science. Gastroenterology 2009;137:1548–1556.
7. Raahave D, Christensen E, Loud FB, et al. Correlation of bowel symptoms with colonic transit, length, and faecal load in functional faecal retention. Dan Med Bull 2009; 56:83–88.
8. Westman EC, Yancy WS, Edman JS, et al. Effect of 6-month adherence to a very low carbohydrate diet program. Am J Med 2002;113:30–36.
9. Dameto MC, Rayo JM, Esteban S, et al. Effect of cafeteria diet on the gastrointestinal transit and emptying in the rat. Comp Biochem Physiol A Comp Physiol 1991; 99:651–655.
10. Nezami BG, Mwangi SM, Lee JE, et al. MicroRNA 375 mediates palmitate-induced enteric neuronal damage and high-fat diet-induced delayed intestinal transit in mice. Gastroenterology 2014;146:473–483 e3.
11. Serino M, Luche E, Gres S, et al. Metabolic adaptation to a high-fat diet is associated with a change in the gut microbiota. Gut 2012;61:543–553.
12. DiBaise JK, Zhang H, Crowell MD, et al. Gut microbiota and its possible relationship with obesity. Mayo Clin Proc 2008;83:460–469.
13. McVey Neufeld KA, Mao YK, et al. The microbiome is essential for normal gut intrinsic primary afferent neuron excitability in the mouse. Neurogastroenterol Motil 2013; 25: 183–e88.
14. Malpeli A, Gonzalez S, Vicentin D, et al. Randomised, double-blind and placebo-controlled study of the effect of a synbiotic dairy product on orocecal transit time in healthy adult women. Nutr Hosp 2012; 27:1314–1319.
15. Ishizuka A, Tomizuka K, Aoki R, et al. Effects of administration of Bifidobacterium animalis subsp. lactis GCL2505 on defecation frequency and bifidobacterial microbiota composition in humans. J Biosci Bioeng 2012;113:587–591.
16. Cani PD, Neyrinck AM, Fava F, et al. Selective increases of bifidobacteria in gut microflora improve high-fat-diet-induced diabetes in mice through a mechanism associated with endotoxaemia. Diabetologia 2007;50: 2374–2383.
17. Jeffery IB, O'Toole PW, Ohman L, et al. An irritable bowel syndrome subtype defined by species-specific alterations in faecal microbiota. Gut 2012;61:997–1006.
18. Jeffery IB, Quigley EM, Ohman L, et al. The microbiota link to irritable bowel syndrome: an emerging story. Gut Microbes 2012;3:572–576.
19. Mujico JR, Baccan GC, Gheorghe A, et al. Changes in gut microbiota due to supplemented fatty acids in diet-induced obese mice. Br J Nutr 2013;110:711–720.
20. Hildebrandt MA, Hoffmann C, Sherrill-Mix SA, et al. High-fat diet determines the composition of the murine gut microbiome independently of obesity. Gastroenterology 2009;137: 1716–1724 e1-2.
21. Wang Y, Devkota S, Musch MW, et al. Regional mucosa-associated microbiota determine physiological expression of TLR2 and TLR4 in murine colon. PLoS One 2010; 5:e13607.
22. Barajon I, Serrao G, Arnaboldi F, et al. Toll-like receptors 3, 4, and 7 are expressed in the enteric nervous system and dorsal root ganglia. J Histochem Cytochem 2009; 57:1013–1023.
23. Ma Y, Li J, Chiu I, et al. Toll-like receptor 8 functions as a negative regulator of neurite outgrowth and inducer of neuronal apoptosis. J Cell Biol 2006;175:209–215.
24. Tang SC, Lathia JD, Selvaraj PK, et al. Toll-like receptor-4 mediates neuronal apoptosis induced by amyloid beta-

peptide and the membrane lipid peroxidation product 4-hydroxynonenal. Exp Neurol 2008;213:114–121.
25. Coquenlorge S, Duchalais E, Chevalier J, et al. Modulation of lipopolysaccharide-induced neuronal response by activation of the enteric nervous system. J Neuroinflammation 2014;11:202.
26. Wang N, Wang H, Yao H, et al. Expression and activity of the TLR4/NF-kappaB signaling pathway in mouse intestine following administration of a short-term high-fat diet. Exp Ther Med 2013;6:635–640.
27. Wang Z, Liu D, Wang F, et al. Saturated fatty acids activate microglia via Toll-like receptor 4/NF-kappaB signalling. Br J Nutr 2012;107:229–241.
28. Huang S, Rutkowsky JM, Snodgrass RG, et al. Saturated fatty acids activate TLR-mediated proinflammatory signaling pathways. J Lipid Res 2012;53:2002–2013.
29. Kuwabara T, Mori K, Mukoyama M, et al. Exacerbation of diabetic nephropathy by hyperlipidaemia is mediated by Toll-like receptor 4 in mice. Diabetologia 2012; 55:2256–2266.
30. Everard A, Lazarevic V, Derrien M, et al. Responses of gut microbiota and glucose and lipid metabolism to prebiotics in genetic obese and diet-induced leptin-resistant mice. Diabetes 2011;60:2775–2786.
31. Chassaing B, Koren O, Carvalho FA, et al. AIEC pathobiont instigates chronic colitis in susceptible hosts by altering microbiota composition. Gut 2013;63:1069–1080.
32. Anitha M, Vijay-Kumar M, Sitaraman SV, et al. Gut microbial products regulate murine gastrointestinal motility via Toll-like receptor 4 signaling. Gastroenterology 2012; 143:1006–1016.e4.
33. Vijay-Kumar M, Aitken JD, Carvalho FA, et al. Metabolic syndrome and altered gut microbiota in mice lacking Toll-like receptor 5. Science 2010;328:228–231.
34. Chandrasekharan BP, Kolachala VL, Dalmasso G, et al. Adenosine 2B receptors (A(2B)AR) on enteric neurons regulate murine distal colonic motility. FASEB J 2009; 23:2727–2734.
35. Miller MS, Galligan JJ, Burks TF. Accurate measurement of intestinal transit in the rat. J Pharmacol Methods 1981; 6:211–217.
36. Srinivasan S, Anitha M, Mwangi S, et al. Enteric neuroblasts require the phosphatidylinositol 3-kinase/Akt/Forkhead pathway for GDNF-stimulated survival. Mol Cell Neurosci 2005;29:107–119.
37. Anitha M, Joseph I, Ding X, et al. Characterization of fetal and postnatal enteric neuronal cell lines with improvement in intestinal neural function. Gastroenterology 2008; 134:1424–1435.
38. Lopaschuk GD, Collins-Nakai R, Olley PM, et al. Plasma fatty acid levels in infants and adults after myocardial ischemia. Am Heart J 1994;128:61–67.
39. Srinivasan S, Bernal-Mizrachi E, Ohsugi M, et al. Glucose promotes pancreatic islet beta-cell survival through a PI 3-kinase/Akt-signaling pathway. Am J Physiol Endocrinol Metab 2002;283:E784–E793.
40. Mushref MA, Srinivasan S. Effect of high fat-diet and obesity on gastrointestinal motility. Ann Transl Med 2013;1:14.
41. Park JH, Kwon OD, Ahn SH, et al. Fatty diets retarded the propulsive function of and attenuated motility in the gastrointestinal tract of rats. Nutr Res 2013; 33:228–234.
42. Rivera LR, Poole DP, Thacker M, et al. The involvement of nitric oxide synthase neurons in enteric neuropathies. Neurogastroenterol Motil 2011;23:980–988.
43. Colucci M, Cervio M, Faniglione M, et al. Intestinal dysmotility and enteric neurochemical changes in a Parkinson's disease rat model. Auton Neurosci 2012; 169:77–86.
44. Stenkamp-Strahm CM, Kappmeyer AJ, Schmalz JT, et al. High-fat diet ingestion correlates with neuropathy in the duodenum myenteric plexus of obese mice with symptoms of type 2 diabetes. Cell Tissue Res 2013; 354:381–394.
45. Beraldi EJ, Soares A, Borges SC, et al. High-fat diet promotes neuronal loss in the myenteric plexus of the large intestine in mice. Dig Dis Sci 2014; 60:841–849.
46. Rivera LR, Leung C, Pustovit RV, et al. Damage to enteric neurons occurs in mice that develop fatty liver disease but not diabetes in response to a high-fat diet. Neurogastroenterol Motil 2014;26:1188–1199.
47. Daniel H, Moghaddas Gholami A, Berry D, et al. High-fat diet alters gut microbiota physiology in mice. ISME J 2014;8:295–308.
48. Cani PD, Amar J, Iglesias MA, et al. Metabolic endotoxemia initiates obesity and insulin resistance. Diabetes 2007;56:1761–1772.
49. Ley RE, Turnbaugh PJ, Klein S, et al. Microbial ecology: human gut microbes associated with obesity. Nature 2006;444:1022–1023.
50. Voss U, Ekblad E. Lipopolysaccharide-induced loss of cultured rat myenteric neurons - role of AMP-activated protein kinase. PLoS One 2014;9:e114044.
51. Voss U, Sand E, Olde B, et al. Enteric neuropathy can be induced by high fat diet in vivo and palmitic acid exposure in vitro. PLoS One 2013;8:e81413.
52. Li J, Chen L, Zhang Y, et al. TLR4 is required for the obesity-induced pancreatic beta cell dysfunction. Acta Biochim Biophys Sin (Shanghai) 2013;45: 1030–1038.
53. Zhou H, Chen D, Xie H, et al. Activation of MAPKs in the anti-beta2GPI/beta2GPI-induced tissue factor expression through TLR4/IRAKs pathway in THP-1 cells. Thromb Res 2012;130:e229–e235.
54. Wang CP, Li JL, Zhang LZ, et al. Isoquercetin protects cortical neurons from oxygen-glucose deprivation-reperfusion induced injury via suppression of TLR4-NF-small ka, CyrillicB signal pathway. Neurochem Int 2013; 63:741–749.
55. He Y, Zhou A, Jiang W. Toll-like receptor 4-mediated signaling participates in apoptosis of hippocampal neurons. Neural Regen Res 2013;8:2744–2753.
56. Czapski GA, Gajkowska B, Strosznajder JB. Systemic administration of lipopolysaccharide induces molecular and morphological alterations in the hippocampus. Brain Res 2010;1356:85–94.

57. Venkataramana S, Lourenssen S, Miller KG, et al. Early inflammatory damage to intestinal neurons occurs via inducible nitric oxide synthase. Neurobiol Dis 2015; 75:40–52.

Received October 13, 2015. Accepted December 24, 2015.

Correspondence
Address correspondence to: Shanthi Srinivasan, MD, Division of Digestive Diseases, Whitehead Biomedical Research Building, 615 Michael Street, Suite 201A, Atlanta, Georgia 30322. e-mail: ssrini2@emory.edu; fax: (404) 727-5767.

Acknowledgment
The authors would like to acknowledge the animal facility in Emory University.

Conflicts of interest
The authors disclose no conflicts.

Funding
This research was funded by National Institutes of Health grant RO1-DK080684 and a VA Merit Award (S.S.).